Dropout dynamics in pulsed quantum dot lasers due to mode jumping

G. S. Sokolovskii, E. A. Viktorov, M. Abusaa, J. Danckaert, V. V. Dudelev, E. D. Kolykhalova, K. K. Soboleva, A. G. Deryagin, I. I. Novikov, M. V. Maximov, A. E. Zhukov, V. M. Ustinov, V. I. Kuchinskii, W. Sibbett, E. U. Rafailov , and T. Erneux

Articles you may be interested in

A dual-mode quantum dot laser operating in the excited state
Appl. Phys. Lett. 99, 231110 (2011); 10.1063/1.3667193

Pulse width narrowing due to dual ground state emission in quantum dot passively mode locked lasers
Appl. Phys. Lett. 96, 211110 (2010); 10.1063/1.3432076

Dynamics of a two-state quantum dot laser with saturable absorber
Appl. Phys. Lett. 90, 121113 (2007); 10.1063/1.2715023
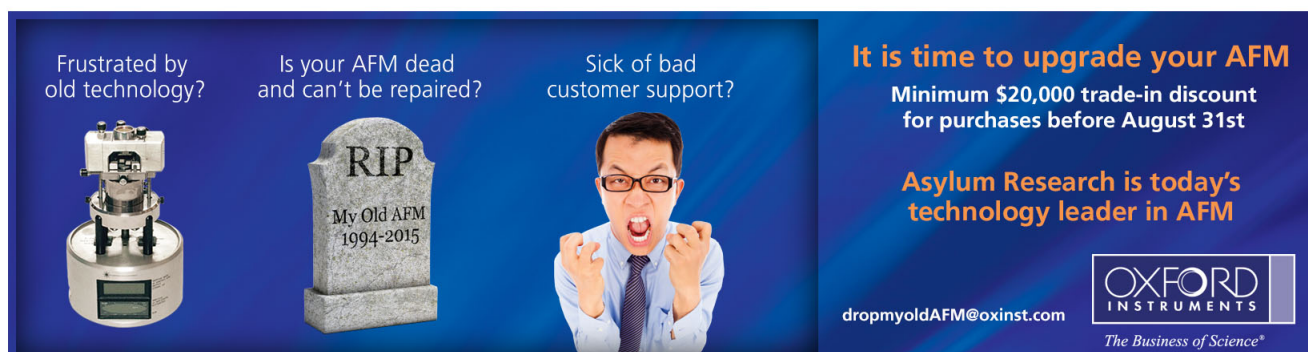
Pulse generation and compression via ground and excited states from a grating coupled passively mode-locked quantum dot two-section diode laser
Appl. Phys. Lett. 89, 261106 (2006); 10.1063/1.2410217

Investigation of transition dynamics in a quantum-dot laser optically pumped by femtosecond pulses
Appl. Phys. Lett. 88, 041101 (2006); 10.1063/1.2166207

Dropout dynamics in pulsed quantum dot lasers due to mode jumping

G. S. Sokolovskii,[1] E. A. Viktorov,[2,3,4] M. Abusaa,[4,5] J. Danckaert,[4] V. V. Dudelev,[1]
E. D. Kolykhalova,[6] K. K. Soboleva,[7] A. G. Deryagin,[1] I. I. Novikov,[1] M. V. Maximov,[1]
A. E. Zhukov,[8] V. M. Ustinov,[1] V. I. Kuchinskii,[1] W. Sibbett,[9] E. U. Rafailov,[10] and T. Erneux[3]

[1]Ioffe Physical-Technical Institute, St. Petersburg, Russia
[2]National Research University of Information Technologies, Mechanics and Optics, Saint Petersburg, Russia
[3]Optique Nonlinéaire Théorique, Campus Plaine CP 231, 1050 Bruxelles, Belgium
[4]Applied Physics Research Group (APHY), Vrije Universiteit Brussel, Pleinlaan 2, B-1050 Brussels, Belgium
[5]Arab American University, Jenin, Palestine
[6]St. Petersburg State Electrotechnical University "LETI," St. Petersburg, Russia
[7]St. Petersburg State Polytechnic University, St. Petersburg, Russia
[8]Academic University, St. Petersburg, Russia
[9]University of St. Andrews, St. Andrews, United Kingdom
[10]Aston Institute of Photonic Technologies, Aston University, Birmingham, United Kingdom

We examine the response of a pulse pumped quantum dot laser both experimentally and numerically. As the maximum of the pump pulse comes closer to the excited-state threshold, the output pulse shape becomes unstable and leads to dropouts. We conjecture that these instabilities result from an increase of the linewidth enhancement factor α as the pump parameter comes close to the excited state threshold. In order to analyze the dynamical mechanism of the dropout, we consider two cases for which the laser exhibits either a jump to a different single mode or a jump to fast intensity oscillations. The origin of these two instabilities is clarified by a combined analytical and numerical bifurcation diagram of the steady state intensity modes. © 2015 AIP Publishing LLC.
[http://dx.doi.org/10.1063/1.4923244]

High-power laser diode operation is an important issue for the laser community since its first demonstration at room temperature.[1] Over the past years, great progress in continuous wave high-power semiconductor lasers was achieved with dramatic reduction of the internal losses. Numerous solutions of the optical damage problem[2] have been proposed that include non-absorbing (with, e.g., intermixing techniques[3]) and non-injecting mirrors,[5] large optical cavity,[4] and aluminum-free laser diode concepts[6] as well as sophisticated facet passivation techniques. On the other hand, short pulsed gain-switched laser operation allows 1–2 orders higher output power due to reduction of the overheating effects. This has motivated the study of high-power pulse generation at pumping level of 10 s to 100 s threshold values. Today, high power pulsed laser diode operation is appealing for multiple biomedical applications including photo-depilation,[7,8] laser liposuction,[9] generation of ceramides[10] and heat-shock proteins,[11] and material processing.[12] In many such applications, quantum dot semiconductor lasers (QDLs) have shown significant advantages as high power pulse generators due to their high gain efficiency and small size.[13]

In this letter, we examine the high power pulsed operation in an electrically pumped QD laser both experimentally and numerically. The output pulse shape is observed to be dependent on the pump current. At lower currents which correspond to lasing at the ground state (GS), the pulse shape mimics that of the pump pulse. At higher currents, the pulse shape becomes progressively unstable. This instability is strongly pronounced in the proximity of the secondary threshold which corresponds to the appearance of the excited state (ES). After a slow rise stage, the output power sharply drops out. It is followed by large-scale amplitude

fluctuations. We explain these observations by the change of the α–factor in QD lasers between the first (GS) and the secondary (ES) threshold. We explore the role of the slowly rising α in the pulse shaping and power dropouts. Slowly varying control parameters may significantly affect the dynamics at bifurcation points. Specifically, the expected bifurcation transition is delayed due to the inertia of the system's response close to bifurcation points. Slow passage problems have been well studied in the nonlinear optics literature.[14,15]

Experimentally, the studied QD laser structure was grown on a GaAs substrate by molecular-beam epitaxy. The active region included five layers of self-assembled InAs QDs separated with a GaAs spacer from a 5.3 nm thick covering layer of $In_{0.14}Ga_{0.86}As$. Finally, the structure was processed into 4 μm-wide mesa stripe devices. The 1.5–2.5 mm long lasers with high- and antireflection coatings on the rear and front facets lase either at the GS (around 1265 nm, $\sim$50 mA threshold at the pulsed pump) or simultaneously at the GS and ES (around 1190 nm, $\sim$1.5 A threshold at the pulsed pump) in the whole range of pumping. Short-pulsed electrical pumping with a total pulse duration of 30 ns was used to achieve high output power operation and avoid the effect of overheating on the output pulse shape. Pulses of $\sim$5 ns rise-time were obtained from a high power digital pulse source (up to 2 A current), and the laser output was detected using a high-speed pin detector with a cut-off frequency of 30 GHz and a 50 GHz digital oscilloscope.

The experimental output pulse shapes and corresponding optical spectra are shown in Fig. 1. We distinguish three different regimes of operation in relation to the ES threshold. In Fig. 1(a), the GS output pulse shape is similar to that of the pulsed pump up to $\sim$0.8 A pump current. It consists of a
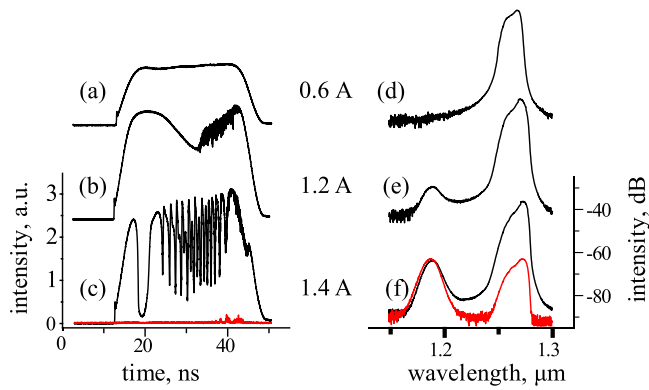
FIG. 1. Experimental time traces (a)–(c) and optical spectra (d)–(f) of the optical output for a range of pump currents: (a) and (d) 0.6 A; (b) and (e) 1.2 A; and (c) and (f) 1.4 A. The solid line represents the total output. The red (bottom) line corresponds to the ES time trace (c) and optical spectrum (f). The laser operates exclusively at the GS for the pump currents below 1.5 A.

~5 ns rise-time, flat operation for ~20 ns, and then a ~5 ns fall time. In Fig. 1(b), the laser operates at approximately 20 GS thresholds and in the proximity of the ES threshold. After the ~5 ns rise stage, the GS output power gradually decreases. It is followed by fast oscillations. At higher currents, closer to the ES threshold (Fig. 1(c)), the laser output at the pulse front first corresponds to the GS. As the pump pulse reaches its top, the output power drops out. It is followed by large amplitude oscillations. The power dropout appears at or even before the end of the 5 ns rise-time.

We conjecture that the change of the pulse profile and the power dropout is related to the dynamical change of the phase amplitude coupling with the pump current. At lower currents, the power dropout phenomenon occurs much later than the rise-time of 5 ns (Fig. 1(b)). At higher currents, close to the ES threshold, the dropout happens when the peak pump power has been reached (Fig. 1(c)). The complicated time evolutions observed after dropouts are difficult to analyze at this stage, and we will mainly concentrate on the origin of the power dropout. The latter will be related to the variations in the phase-amplitude coupling of the field with the increase of the pump current.

In a conventional semiconductor laser, the phase-amplitude coupling is characterized by the $\alpha-$factor.[16] Its impact on laser performance has been a subject of intensive research for decades. Measurements of the $\alpha-$factor in a QD laser are not so well documented. It has been shown that various measurement techniques can lead to different values of the $\alpha-$factor.[17] Numerical results presented in Refs. 18 and 19 suggest a complex dynamics of the $\alpha-$ factor in QD lasers. Experimental results for simultaneous GS/ES lasing[20] reveal that by contrast to conventional semiconductor lasers, the $\alpha-$factor in QD lasers significantly increases above the GS threshold, and a value $\alpha = 57$ was measured just below the ES threshold. Direct measurement of the $\alpha-$factor cannot be performed for the pulse pumped laser as all known techniques (except for extraction from the amplified spontaneous emission, which is applicable near threshold) rely on cw laser operation which cannot be experimentally achieved for the high pump currents (up to 1.5 A, 50-fold cw threshold) that have been used in our experiments. The dynamical effects in our work appear at extremely high currents (>1 A)

when the laser operates close to full inversion. This case has been considered theoretically in Ref. 17, and strong dependence of the $\alpha-$factor on the current has been demonstrated. The increase of $\alpha-$factor with pump current in QD lasers has also been reported in Refs. 21 and 22, and is the key assumption in our modeling.

In order to describe the experimental observation, we consider a delay differential equation (DDE) model[23] with dynamical $\alpha-$factor. The DDE approach supports multimode generation which is essential to describe the dropout. Our objective is mainly to clarify the origin of the power dropout, and we do not consider the ES in this model. The model consists of the following three equations:

$$\gamma^{-1}E'(t) + E(t) = \sqrt{\kappa}[e^{(1-i\alpha(t))G(t-T)/2}]E(t-T), \quad (1)$$

$$\rho'(t) = \eta[-\rho + BN(1-\rho) - [e^G - 1]|E|^2], \quad (2)$$

$$N'(t) = \eta[J(t) - N - 2BN(1-\rho)], \quad (3)$$

where prime means differentiation with respect to $t \equiv t'/\tau_{ph}$, where t' is time and $\tau_{ph} = 10$ ps is the photon lifetime. $\eta \equiv \tau_{ph}\tau^{-1} = 10^{-2}$, where $\tau = 1$ ns denotes the carrier recombination time. E is the normalized electric field, ρ is the occupational probability in the ensemble of QDs, and N is the 2D carrier density in the wetting layer (WL). The gain $G = 2g$ $(2\rho - 1)$ is defined by the dot population and a g-factor, which we define as the effective gain factor. The term $BN(1-\rho)$ describes phonon-assisted capturing of the carriers from the wetting layer into the dot limited by the Pauli blocking factor. $B \equiv \tau\tau_{cap}^{-1} = 10^2$, where $\tau_{cap} = 10$ ps denotes the capture time. The factor 2 accounts for the degeneracy in the quantum dot energy levels. $T = T'/\tau_{ph}$ is the dimensionless laser cavity round trip time. With $T' = 10 - 20 ps$, $T = 1 - 2$. The attenuation factor $\kappa = 0.3$ describes the total non-resonant linear intensity losses per cavity round trip. $\gamma = \gamma'\tau_{ph}$ is the dimensionless bandwidth of the optical spectrum. With $1/\gamma' = 1 - 3 ps$, $\gamma = 10 - 30$. J is the pump current per dot, and is a function of time. The pulse pump has a $\tau_{rf} = 5$ ns rise (fall) time and then reaches a plateau equal to J_0. The plateau duration is $\tau_{pl} = 20$ ns. In dimensionless form,

$$J(t) = \frac{t}{t_{rf}} (0 \leq t < t_{rf}),$$
$$= J_0(t_{rf} \leq t \leq t_{rf} + t_{pl}), \quad (4)$$
$$= J_0 \left(1 - \frac{t - t_{rf} - t_{pl}}{t_{rf}}\right)(t_{rf} + t_{pl} < t \leq 2t_{rf} + t_{pl}),$$

where $t_{rf} = \tau_{rf}/\tau_{ph} = 500$. We propose that the $\alpha-$factor depends on the cavity, and the gain variations caused by the pump current increase and the optothermal effects. In order to describe the evolution of alpha, we introduce

$$\gamma_\alpha^{-1}\alpha' = -\alpha + \hat{\alpha} + \beta|E|^2, \quad (5)$$

where $\gamma_\alpha^{-1} = 1000 \gg \gamma^{-1}$ is the slow relaxation rate. $\hat{\alpha} = 1$ is the value of the $\alpha-$factor in the absence of the pump current effects, and β is an amplitude of the intensity dependence. We take into account the limited bandwidth of the experimental detection by introducing a filtered intensity satisfying

$$I' = \frac{1}{t_f}\left(|E|^2 - I\right), \qquad (6)$$

where $t_f = \tau_f/\tau_{ph}$ is the dimensionless time constant of the filter taken as $t_f = 10$ for the simulations in Figs. 2 and 3.

The dimensionless equations (1)–(3) facilitate the numerical simulations and are needed for our analytical work. We will, however, display the numerical simulations in terms of the original time for best comparison with the experiments. Some examples of the filtered intensity are shown in Fig. 2 for a range of the pumping amplitude J_0. At low J_0, the output pulse is similar to the pump pulse (Fig. 2(a)). At higher J_0, the intensity also follows the pump temporal evolution at the front of the pulse, but either slowly decreases or sharply drops (Figs. 2(b) and 2(c)). The power dropout is followed by fast large-amplitude oscillations. It corresponds to the experimental observations at higher currents.

QD lasers are known as complicated systems exhibiting different time scales.[24] The turn-on dynamics has recently been investigated in detail.[25,26] but a slow increase of the pump current is a different process. We note that the lasing modes do not emerge simultaneously, but sequentially appear as the pump current increases. As a result, the change of the α−factor leads to significant spectral shifts in the position of the lasing modes. The α−factor in Fig. 2 slowly rises similar to the evolution of the pump current, and remains nearly constant after that.

We investigate the effect of the slowly varying pump by analyzing Eqs. (1)–(3) in the simplest case where the maximum gain mode admits a bifurcation transition either to another single mode or to a two mode regime. The
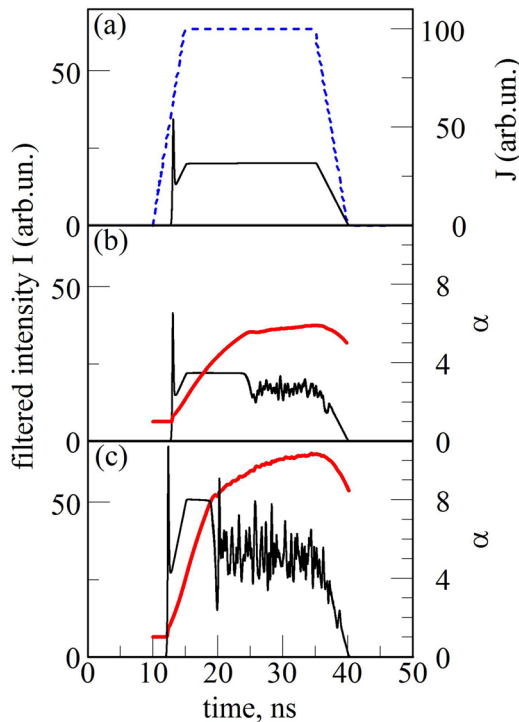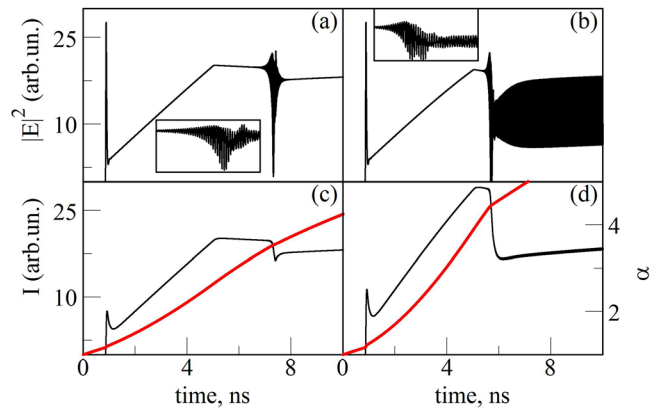

FIG. 3. Unfiltered (a) and (b) and filtered (d) and (c) time traces illustrating the transition from the unstable maximum gain mode to (a) and (c) another single mode ($\beta = 0.2$) or to (b) and (d) a two mode beating ($\beta = 0.5$). The red (thick) line in (c) and (d) shows the evolution of the α−factor. The parameters are $g = 2, T = 1, \gamma = 10, J_0 = 100, \eta = 10^{-2}, B = 10^2, \kappa = 0.3$. Insets show the transitions in more detail. The beating effect is only weakly pronounced in filtered traces (d).

bifurcations are noted by either a slow transient or by a sharp power dropout. These dynamics are shown in Fig. 3. After the laser turns on (damped fast oscillations), the laser output follows the lasing state at the maximum gain mode. At a certain value of $J(t)$, this mode becomes unstable, but the transition to another single mode mode (Figs. 3(a) and 3(c)) or a two mode regime (Figs. 3(b) and 3(d)) is happening with a certain delay. The transition consists of two stages. At the first stage, the unstable maximum gain mode output evolves in a spiral motion (shown in the insets of Fig. 3(a) and 3(b)). At the second stage, the spiral drifts towards another attractor which is either a stable focus (single mode in Fig. 3(a)) or a limit-cycle (two mode beating in Fig. 3(b)).

We next wish to substantiate our numerical observations by an analysis of the cavity modes (CMs) of Eqs. (1)–(3) with constant $\alpha = \alpha_0$. Using the decomposition $E = R\exp(i\omega t)$ and assuming $R, \omega, G,$ and N constants, we found a parametric solution with ω as the parameter. Specifically, we progressively change ω and first compute $G(\omega)$ as

$$G = \ln[(1 + (\gamma^{-1}\omega)^2)/\kappa]. \qquad (7)$$

We then determine $\alpha_0 = \alpha_0(\omega)$ from

$$\alpha_0 = \frac{2}{G}\left[-\omega T - \arctan(\gamma^{-1}\omega) + n\pi\right], \qquad (8)$$

where n is an even integer that defines a cavity mode (CM). Together with (7), we obtained a parametric solution for ω and G now as a function of α_0 and n. Finally, we compute N and R^2 using

$$N = \frac{J}{1 + 2B(1 - \rho)}, \qquad (9)$$

$$R^2 = \frac{-\rho + BN(1 - \rho)}{\exp(G) - 1} \geq 0. \qquad (10)$$

The modal intensities R^2 and frequencies ω are parametrically determined using Eqs. (7)–(10). A numerical

FIG. 2. Numerical time traces illustrating the effect of an increasing α−factor on the pulse profile: (a) $J_0 = 100$, (b) $J_0 = 110$, and (c) $J_0 = 250$. The blue (dotted) line in (a) corresponds to the pump pulse. The red (thick) line in (b) and (c) shows the evolution of the α−factor. The parameters are $g = 0.8, \beta = 0.3, T = 2, \gamma = 30, \eta = 10^{-2}, B = 10^2, \kappa = 0.3$.

bifurcation diagram is shown in Fig. 4 and illustrates the interplay between the different CMs obtained for a range of α_0. At smaller α_0, the laser operates at the maximum gain CM$_0$. By progressively increasing α_0, we observe a jump to CM$_2$ near $\alpha_0 = 3$. The jump appears after a subcritical Hopf bifurcation and corresponds to the power dropout in the numerical time trace (Figs. 3(a) and 3(b)). It explains the experimental observation as a sharp dynamical deformation of the modal structure caused by a change of the amplitude-phase coupling in the vicinity of the ES.

The transient motion shown in Fig. 3(a) corresponds to a mixed mode regime appearing during the jump transition. The system remains locked to CM$_2$ as α_0 further increases. By decreasing α_0 from $\alpha_0 = 8$, we observe a stable time-periodic solution that disappears near $\alpha_0 = 2$. Its time trace exhibits nearly harmonic oscillations with a period close to 2π and suggest a beating between CM$_0$ and CM$_2$ of the form

$$E \simeq R_0 \exp(i\omega_0 t) + R_2 \exp(i\omega_2 t + \phi), \quad (11)$$

implying an intensity $|E|^2 = R_0^2 + R_2^2 + 2R_0R_2 \cos((\omega_2 - \omega_0)t + \phi)$. We have verified that $\omega_2 - \omega_0$ remains close to 2π as we change α_0 and is exactly 2π at the point where branches CM$_0$ and CM$_2$ intersect. Mathematically, we may anticipate that the branch of the two-mode solution (11) connects two single Hopf bifurcation points located on each interacting single mode. This can be demonstrated by an asymptotic analysis valid in the limit $\eta \to 0$ as shown in Ref. 27 and 28 for a simpler laser problem. We have verified numerically that the single mode Hopf bifurcation points indeed converge to the CM$_0$–CM$_2$ crossing point as $\eta \to 0$ (see Fig. 5). They have been determined numerically by changing α_0 forward and backward. For each value of η, we note that the main CM$_0$ admits a subcritical Hopf bifurcation that is causing a sudden jump transition.

In conclusion, we have found that the slow rise time of the pulsed pump may significantly affect the high intensity output pulse in a quantum dot laser. It leads to sharp power

FIG. 5. Bifurcation diagram of the CMs showing two Hopf bifurcation points corresponding to the jump-down and jump-up transition (as indicated by the arrows) as we either increase or decrease α, respectively. (a) $\eta = 5 \times 10^{-3}$. (b) $\eta = 10^{-3}$. (c) $\eta = 5 \times 10^{-4}$. As η becomes smaller, the two Hopf bifurcation points converge to the crossing points (encircled). All other parameters are the same as in Fig. 4.

drops and drastic changes of the pulse profile. We relate this phenomenon to the dynamical change of the phase-amplitude coupling (α-factor). The delay differential equation modeling simulates the experimental observations. A combined analytical and numerical investigation of the bifurcation diagram unveils a beating mechanism between nearby CMs that generates Hopf bifurcation points responsible for fast transitions between CMs, causing dropouts.
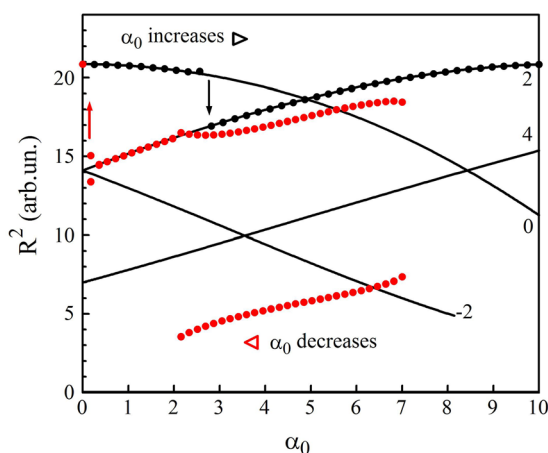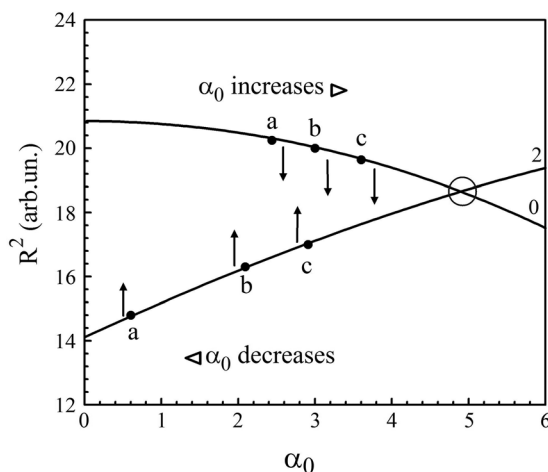
FIG. 4. Bifurcation diagram of the stable steady and periodic intensities. The full lines (dots) are the lasing modes obtained analytically (numerically). They are labeled by their value of n. The diagram has been obtained by either progressively increasing α or decreasing α by steps. At each step, the evolution equations have been integrated for a long time. The intial conditions for the first point are ($E = x + iy$): $x = y = 1$, $\rho = 0.4$ for the interval $-1 \leq s \leq 0$ and $N(0) = 1$. All other parameters are documented in Fig. 3.

[1] Zh. I. Alferov, V. M. Andreev, E. L. Portnoy, and M. K. Trukan, Sov. Phys. Semicond. **3**, 1107 (1970).

[2] P. G. Eliseev, J. Lumin. **7**, 338 (1973); J. W. Tomm, M. Ziegler, M. Hempel, and T. Elsaesser, Laser Photonics Rev. **5**, 422 (2011).

[3] C. L. Walker, A. C. Bryce, and J. H. Marsh, IEEE Photonics Technol. Lett. **14**, 1394 (2002).

[4] D. Botez, Appl. Phys. Lett. **74**, 3102 (1999).

[5] T. Shibutani, M. Kume, K. Hamada, H. Shimizu, K. Itoh, G. Kano, and I. Teramoto, IEEE J. Quantum Electron. **23**, 760 (1987).

[6] D. Z. Garbuzov, N. Y. Antonichkis, A. D. Bondarev, A. B. Gulakov, S. N. Zhigulin, N. I. Katsavets, A. V. Kochergin, and E. U. Rafailov, IEEE J. Quantum Electron. **27**, 1531 (1991).

[7] V. B. Campos, C. C. Dierickx, W. A. Farinelli, T. Y. D. Lin, W. Manuskiatti, and R. R. Anderson, J. Am. Acad. Dermatol. **43**, 442 (2000).

[8] I. Greppi, Lasers Surg. Med. **28**, 150 (2001).

[9] P. Chen, 13th Annual Meeting of the American Society of Breast Surgeons, Phoenix, 2-6 May 2012.

[10] H. Y. Zhang, L. Zhang, P. Tidemand-Lichtenberg, P. Buchhave, X. B. Xu, and Y. X. Li, Photochem. Photobiol. **87**(1), 131 (2011).

[11] G. S. Sokolovskii, S. B. Onikienko, K. K. Soboleva, A. V. Zemlyanoi, N. A. Pikhtin, I. S. Tarasov, B. A. Margulis, and I. V. Guzova, J. Phys.: Conf. Ser. **572**, 012017 (2014).

[12] W. Qin, Y. Liu, Y. Cao, J. Gao, F. Pan, and Z. Wang, Proc. SPIE **8197**, 81971J (2011).

[13]E. U. Rafailov, M. A. Cataluna, and W. Sibbett, Nat. Photonics **1**, 395 (2007).

[14]T. Erneux and P. Glorieux, *Laser Dynamics* (Cambridge University Press, Cambridge, UK, 2010).

[15]M. C. Torrent and M. San Miguel, Phys. Rev. A **38**, 245 (1988).

[16]C. H. Henry, IEEE J. Quantum Electron. **18**, 259 (1982).

[17]S. Melnik, G. Huyet, and A. Uskov, Opt. Express **14**, 2950 (2006).

[18]E. Gehrig and O. Hess, Appl. Phys. Lett. **86**, 203116 (2005).

[19]B. Lingnau, K. Lüdge, W. W. Chow, and E. Schöll, Phys. Rev. E **86**, 065201 (2012).

[20]B. Dagens, B. A. Markus, J. X. Chen, J.-G. Provost, D. Make, O. Le Gouezigou, J. Landreau, A. Fiore, and B. Thedrez, Electr. Lett. **41**, 323 (2005).

[21]A. Martinez, A. Lemaître, K. Merghem, L. Ferlazzo, C. Dupuis, A. Ramdane, J.-G. Provost, B. Dagens, O. Le Gouezigou, and O. Gauthier-Lafaye, Appl. Phys. Lett. **86**, 211115 (2005).

[22]A. Markus, J. X. Chen, O. Gauthier-Lafaye, J.-G. Provost, C. Paranthoën, and A. Fiore, IEEE J. Sel. Top. Quantum Electron. **9**, 1308 (2003).

[23]E. A. Viktorov, P. Mandel, and G. Huyet, Opt. Lett. **32**, 1268 (2007).

[24]T. Erneux, E. A. Viktorov, and P. Mandel, Phys. Rev. A **76**, 023819 (2007).

[25]G. S. Sokolovskii, V. V. Dudelev, E. D. Kolykhalova, A. G. Deryagin, M. V. Maximov, A. M. Nadtochiy, V. I. Kuchinskii, S. S. Mikhrin, D. A. Livshits, E. A. Viktorov, and T. Erneux, Appl. Phys. Lett. **100**, 081109 (2012).

[26]K. Lüdge and E. Schöll, IEEE J. Quantum Electron. **45**, 1396 (2009).

[27]T. Erneux, F. Rogister, A. Gavrielides, and V. Kovanis, Opt. Commun. **183**, 467 (2000).

[28]D. Pieroux, T. Erneux, B. Haegeman, K. Engelborghs, and D. Roose, Phys. Rev. Lett. **87**, 193901 (2001).